

# Development of industrial PCM heat storage prototype



#### DEVELOPMENT OF INDUSTRIAL PCM HEAT STORAGE PROTOTYPE

H.A. Zondag<sup>1</sup>, R. de Boer<sup>1</sup>, S.F. Smeding<sup>1</sup>, J. van der Kamp<sup>2</sup>

<sup>1</sup>ECN Energy reserach Centre of the Netherlands, P.O.Box 1, 1755LE Petten, the Netherlands

<sup>2</sup>Bronswerk Heat Transfer, P.O. Box 92, 3860 AB, Nijkerk, The Netherlands

#### **Abstract**

A 140 liter lab scale shell-and-tube PCM heat storage was built and tested, and the experimental results were compared to a numerical model. Natural convection in the PCM was found to significantly influence the temperature distribution in the storage vessel. A horizontal orientation was found to be beneficial due to increased heat exchange during charging (melting).

#### 1. Introduction

Heat storage can be applied to increase industrial energy efficiency and reduce installation costs, by providing peak heating demand, by storing intermittent waste heat for later use and by decoupling of thermal and electrical yield of CHP systems. In the Dutch project "LOCOSTO", the feasibility of high temperature PCM (Phase Change Material) heat storage is investigated for storage of industrial waste heat in the temperature range between 70°C and 200°C. The focus is on stationary PCM heat storage applications on industrial sites, focusing on heat storage combined with CHP, recuperation and re-use of waste heat from batch processes and emergency backup heating.

Industrial heat storage systems are typically designed for high power, high energy content, high reliability and high temperature, setting specific requirements for PCM materials and PCM additives. In addition, economic return times should be short, which is the more stringent since industrial energy prices are relatively low. Therefore, as much as possible, use is made of low cost and proven industrial components in the upscaling from labscale prototypes to industrially relevant scale, as well as relatively low cost PCM materials.

The present research focuses on thermal design of PCM storage. This thermal design is realized in a cooperation between ECN and Bronswerk Heat Transfer. The PCM storage design is based on a shell and tube heat exchanger, being an industrial standard solution, in which the shell side is filled with the PCM. This introduces a number of design parameters, such as pitch and number of tubes, depending on the effective conductivity of the PCM.

The main aim of the project is to develop and validate a numerical model, that can be used for further upscaling of the design of a PCM storage.

## 2. Modelling heat transfer

A model has been developed in matlab, to calculate the thermal power of a shell-and-tube geometry, for a shell filled with PCM and the tubes carrying the heat transfer medium. The model is suitable of calculating the time dependent thermal power and state of phase for different amounts of tubes, tube pitches and tube lengths.

The matlab model is based on the following assumptions:

- 1) In the PCM, only conductive heat transfer is calculated. Convection in the molten PCM is not explicitly calculated, but corrected for by assuming a higher effective heat exchange between adjacent numerical grid cells containing PCM in liquid state.
- 2) The calculation focuses on a representative segment of the shell-and-tube geometry (typically a quarter of a tube, see Figure 1). Because of this choice, the effect of heat loss from the surface of the tank to the ambient is not taken into account. The boundary condition over the symmetry plane between tubes (blue line in Figure 1b) is set by assuming inversely symmetric boundary conditions  $(T_{1,y} = T_{x,y}, T_{2,y} = T_{x-1,y}, \text{ etc.})$ . In the calculations, usually a grid of radial×axial×tangential= $10 \times 10 \times 10$  cells was used.
- 3) Heat transfer in the PCM is only in the radial direction. Only via the heating up of the tube flow, the longitudinal direction is taken into account. Heat transfer between tangentially connected cells is ignored, which is of some importance as the radial direction changes in length, making the system asymmetric in the tangential direction.

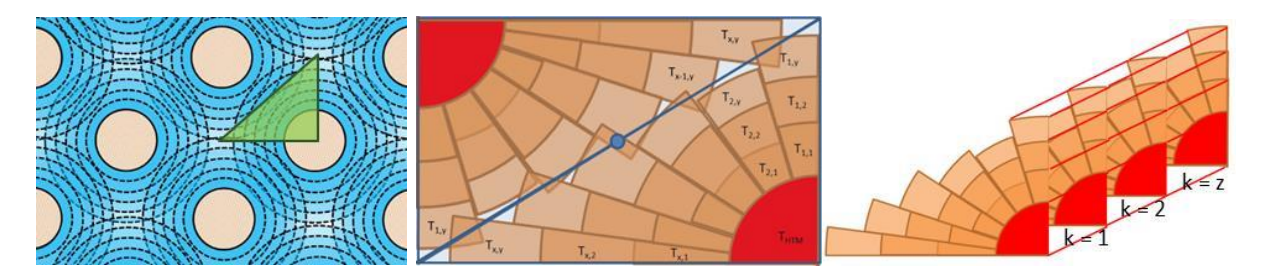


Figure 1: Grid layout of shell-and-tube matlab model.

In order to validate the model, a comparison was made with an analytical solution for a single tube with PCM at the outside. According to Mehling and Cabeza (2008), the analytical solution for this case is:

$$t = \frac{\rho \Delta H}{2\lambda \Delta T} s^2 \times \left( \left( 1 + \frac{R}{s} \right)^2 \ln \left( 1 + \frac{s}{R} \right) - \left( \frac{1}{2} + \frac{R}{s} \right) \right)$$

Note that this equation takes into account only the melting heat; the sensible heat (which is relatively small for a small temperature range) is ignored. From this equation, the power can be determined according to

$$q = \rho \Delta H \frac{ds}{dt} \times 2\pi RL$$

Figure 2 shows a comparison of the storage power calculated by the analytical solution and by the numerical model, for the case of a high flow rate (keeping the temperature in the tube effectively constant in the flow direction). As can be seen, for the case of large pitch and also initially for the case of small pitch, the results from the analytical solution and the model are almost identical. After 1000 s, for small pitch, the solidification front of the tubes starts to overlap, strongly reducing the power that can be extracted.

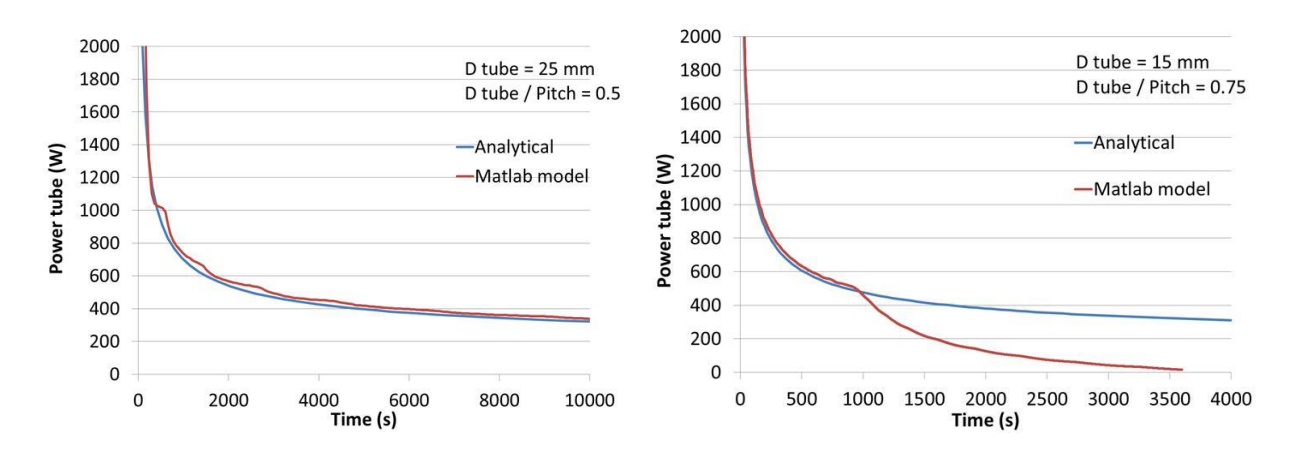


Figure 2: Power versus time (a) Pitch 50 mm (tubes of 6 m length and 25 mm diameter), (b) Pitch 20 mm (tubes of 6 m length and 15 mm diameter).

Also, the model performance was compared qualitatively to the results found in a small lab prototype PCM storage. This lab prototype was built based on a shell-and-tube configuration with 5 tubes, as shown in Figure 3. Geometry-induced inhomogeneities and differences in solidification of organic PCM and salt hydrates were observed. The comparison with the model is shown in Figure 4, indicating a good correspondence between lab prototype and model.



Figure 3: Small scale transparent prototype (a) side view, (b) bottom view, showing the progressing melting front around the tubes.

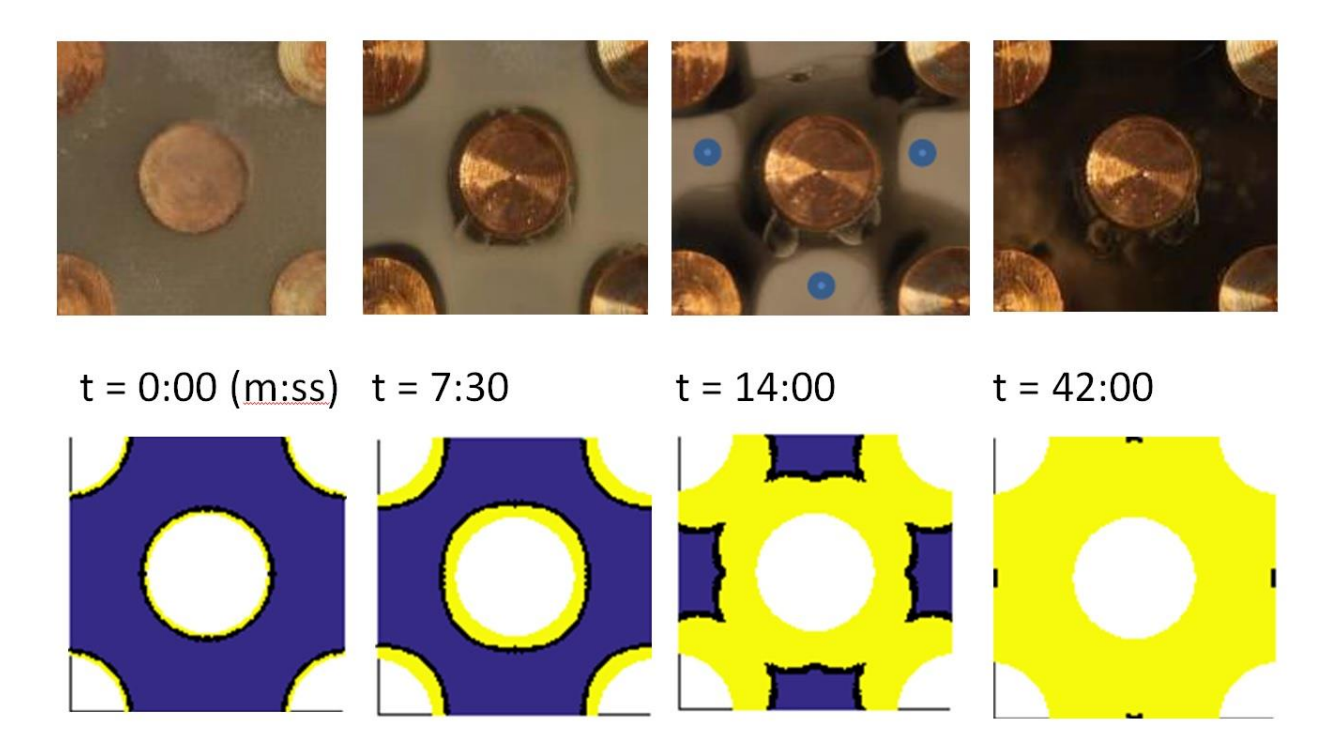


Figure 4: Qualitative comparison of progress of melting front in model and in transparent lab prototype.

### 3. Large scale lab prototype

Next, a large scale lab prototype was built with an internal shell volume of 142 liters to be filled with PCM. The heat exchanger is shown in Figure 5. It contains 49 U-tubes for heat transfer, with an outside diameter of 12 mm and a triangular pitch of 36 mm. The full prototype is shown in Figure 6. The design allows the vessel to be placed in either horizontal or vertical position, to allow for investigation of the orientation of the vessel on natural convection in the molten PCM. In horizontal orientation, the prototype could be filled with 103 kg of paraffine PCM RT70 (in vertical orientation, a slightly lower PCM content of 85 kg was realized, due to limitations caused by the position of the filling valve).

The vessel was connected to a heating/cooling infrastructure, as shown in Figure 6. The inflow temperature to the vessel was controlled by a thermostatic bath, with sufficient cooling/heating power to have an inlet temperature stable within 0.5K of the setpoint value.

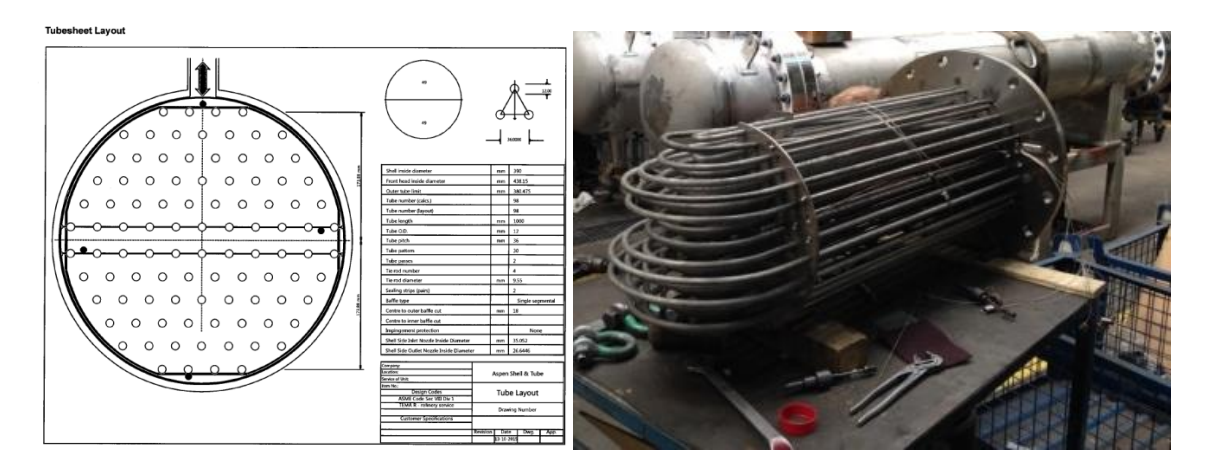


Figure 5 (a) Heat exchanger design, (b) Heat exchanger (before integration in storage vessel).



Figure 6: Large scale prototype (a) horizontal configuration, (b) vertical configuration (after insulation).

Experiments were carried out to validate the numerical model, using detailed measurements on the progress of the melting front between the tubes. The thermocouple distribution is shown in Figure 7. Temperature measurements are carried out both along the reference tube, and in between two tubes, as shown Figure 7b.

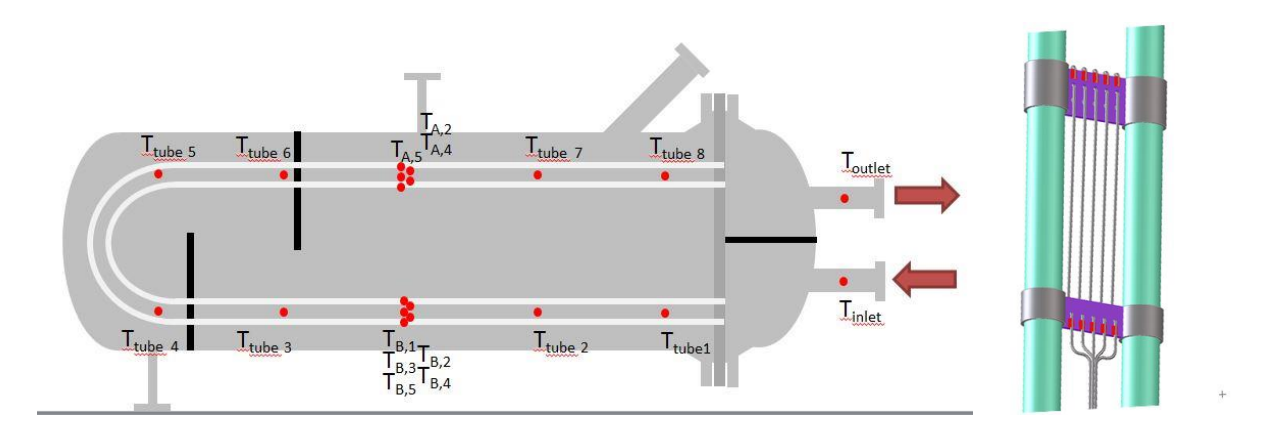


Figure 7: (a) Positioning of thermocouples in vessel, (b) zoom in on thermocouple T108-T112.

For the further analysis of the results, first an assessment was made of the vessel heat loss coefficient (in W/K), by filling the vessel with heated water and measuring the relation between supplied heating power and stabilized vessel temperature. Subsequently, the applied charging and discharging power were corrected for this heat loss, to be able to compare the results to the numerical model (that does not include heat loss).

#### 4. Results and discussion

First, measurements were carried out to examine the results under reference conditions (horizontal orientation, horizontal orientation vessel,  $dT_{PCM-flow}=10^{\circ}C$ , mass flow 20kg/min). Here,  $dT_{PCM-flow}$  is defined as the temperature difference between the PCM melting temperature (as specified by the manufacturer) and the inflow temperature of the heat transfer medium into vessel, as set by the thermostatic bath. Detailed results on the progress of the melting front are shown in Figure 8 (along the tube) and Figure 9 (perpendicular to flow between two tubes). Along the tube, a good qualitative match is found between experiments (solid lines) and model results (dotted lines). The experimental front is sharper than the modelling front, which is related to the limited number of numerical segments in the flow direction. However, quantitatively, the melting and solidification of the PCM occur faster than indicated by the model, indicating the progression of a melting front in the flow direction along the tube. In the direction perpendicular to the tube, the experimental temperature differences seem much smaller than expected based on the model, particularly in the melting phase. This is consistent with the passing of the melting front along the tube as was observed in Figure 8, and seems related to natural convection in the molten PCM, reducing the temperature difference between different locations in the melt. Finally, a double solidification phase was found during the discharge, which is consistent with manufacturer data for this PCM (indicating a double solidification peak at  $70^{\circ}C$  and  $67^{\circ}C$ ).

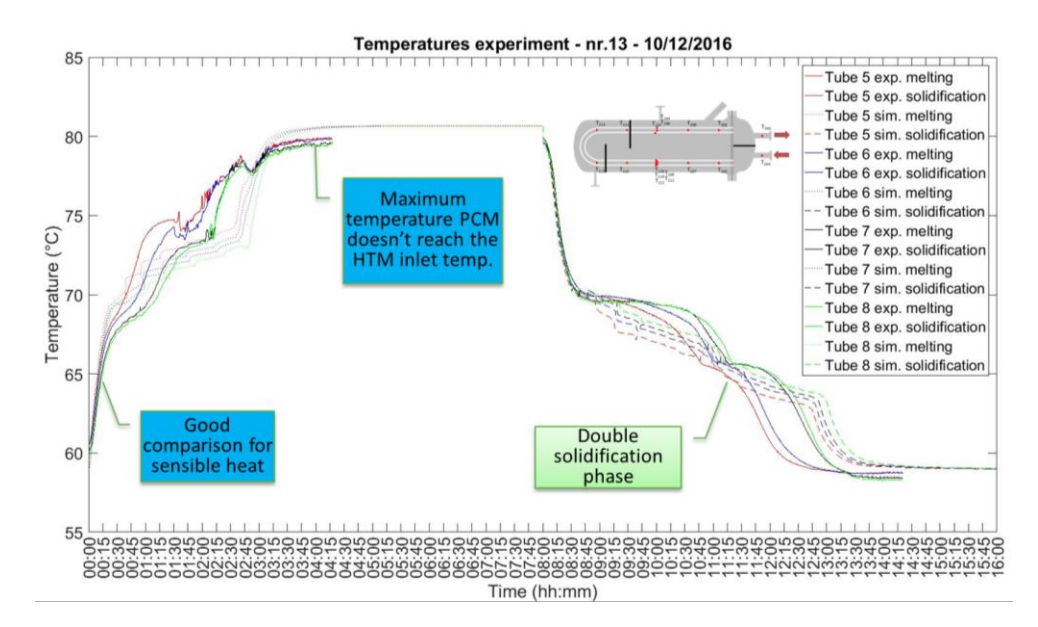


Figure 8: Progress of the melting front along a tube (top section of the tank,  $5 \rightarrow 8$  towards the outlet).

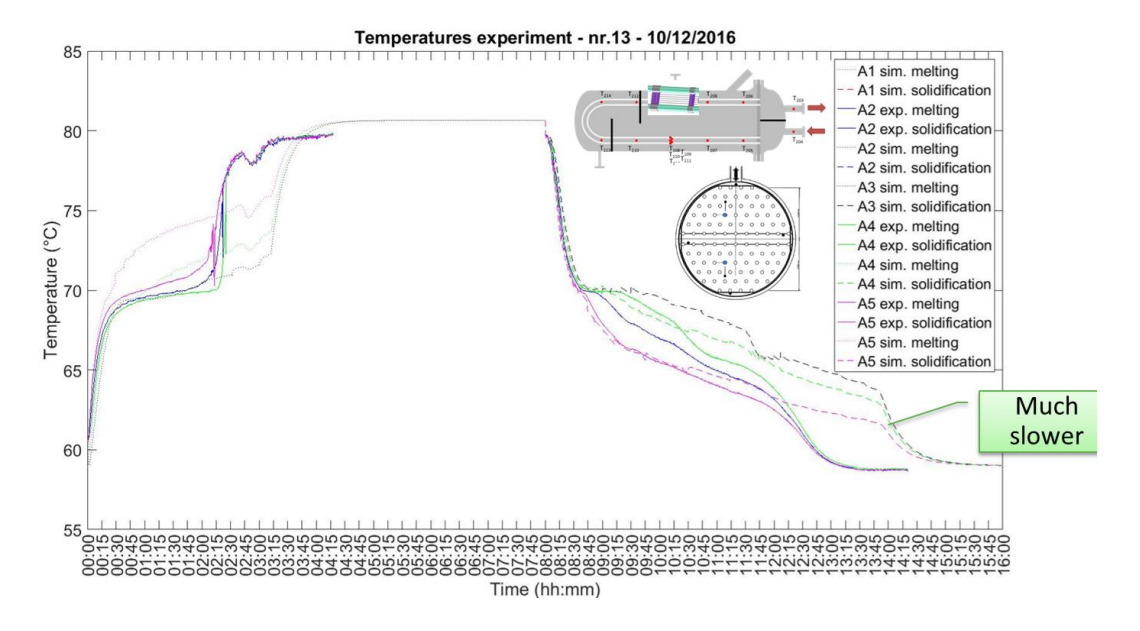


Figure 9: Progress of the melting front between the tubes (top section of the tank).

Figure 10 shows a comparison between the thermal power as calculated by the model and the measurements. The figure shows that on discharge (solidification), the match between model and experiments is good. However, on charging (melting), the experimental storage is charged faster than predicted by the model. This is attributed to the effect of natural convection in the molten PCM, which affects the melting phase much more strongly than the solidification phase. To correct for this, a high effective heat transfer of 150 W/m²K was assumed in the numerical model between cells containing molten PCM, which gives a much better match with the experimental data in the charging phase (as shown in Figure 10), while having almost no effect in the discharging phase (as expected).

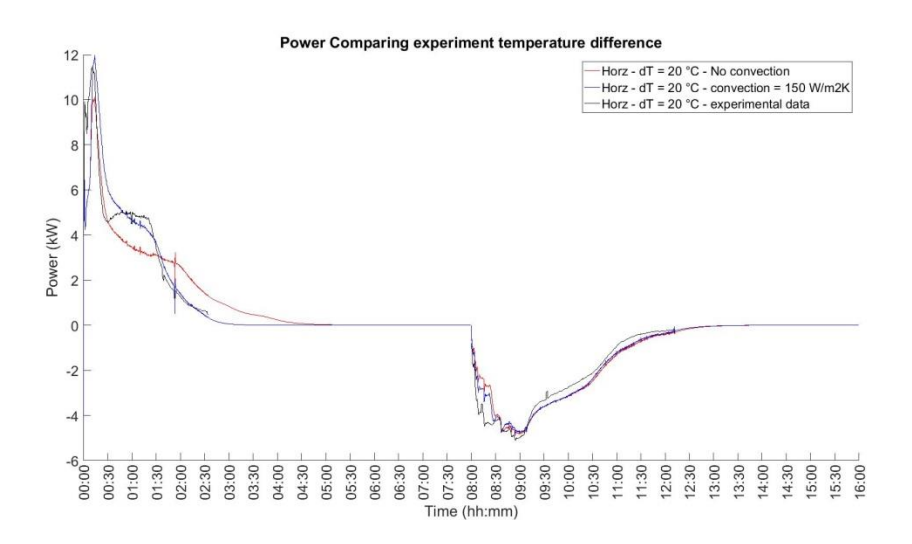


Figure 10: Comparison of power in numerical model with and without correction for PCM convection. (Rubitherm RT70, horizontal orientation vessel, dT=20°C, mass flow 20kg/min).

Figure 11 shows the experimental and numerical energy balance. With the natural convection correction in the model, the charging and discharging are now predicted very well.

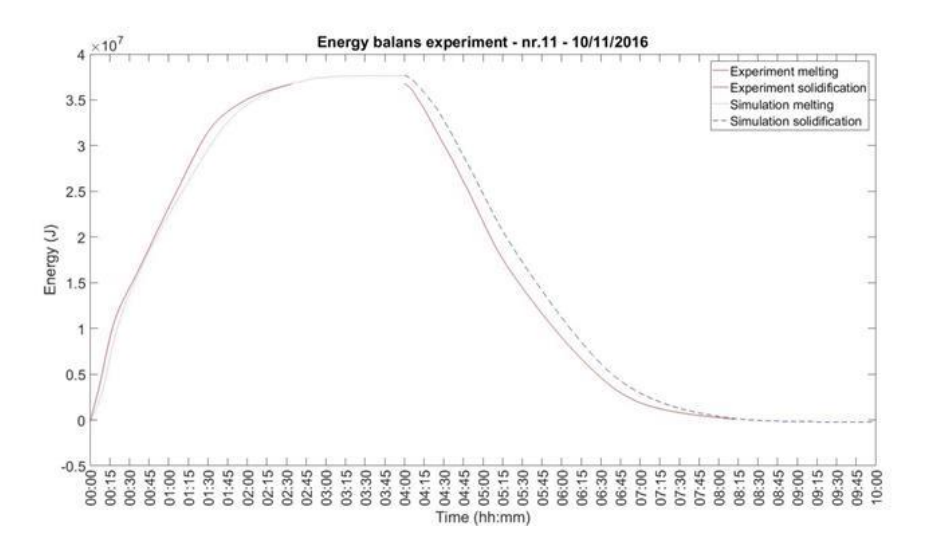


Figure 11: Comparison between energy balance in model (including natural convection correction term) and in experimental setup (Rubitherm RT70, horizontal orientation vessel, dT=20°C, mass flow 20kg/min).

To investigate the performance of the PCM heat storage, a number of settings were varied, in particular the flow rate of the heat transfer medium that was thermally charging and discharging the storage, the effect of the temperature difference between the heat transfer medium and the PCM, and finally the effect of orientation of the storage (which affects the natural convection in the molten PCM).

Figure 12 shows the energy balance for various temperature differences between PCM and heat transfer fluid. The instantaneous energy content was scaled to the maximum energy content under the given conditions, to be able to compare the results for the different settings. Clearly, higher temperature differences cause faster charging and discharging of the storage. A similar but smaller effect can be found in Figure 13, in which a larger mass flow causes higher charge and discharge power. This is to be expected, because the higher mass flow reduces the temperature change in the heat transfer medium along the flow direction, increasing the effective temperature difference between fluid and PCM along the tube. Nevertheless, the effect is relatively small, indicating that the flow speeds used are not the rate limiting factor in the performance of the storage; the thermal conductivity of the PCM is still the limiting factor. However, this could change on further reduction of the flowrate.

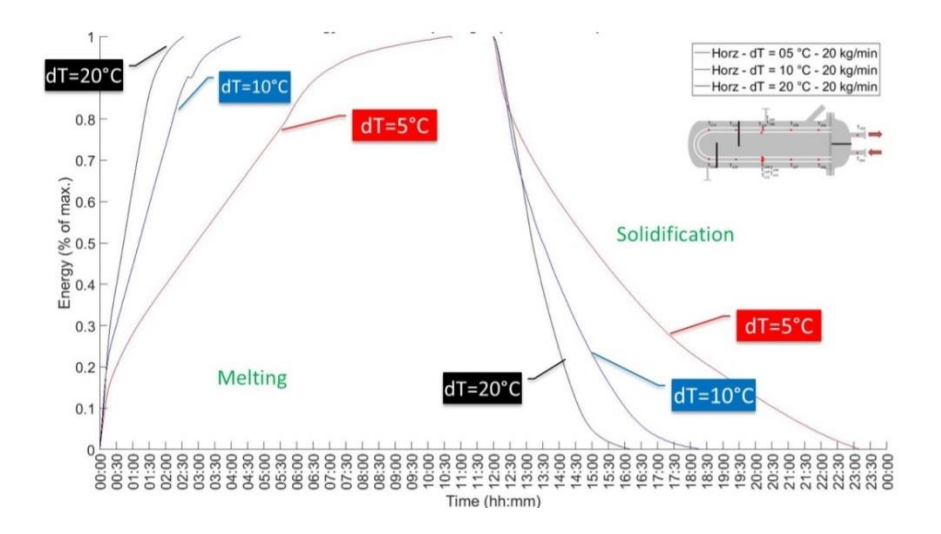


Figure 12: Effect of temperature difference on energy content of storage for charging and discharging. Flow rate is 20 kg/min, vessel orientation is horizontal.

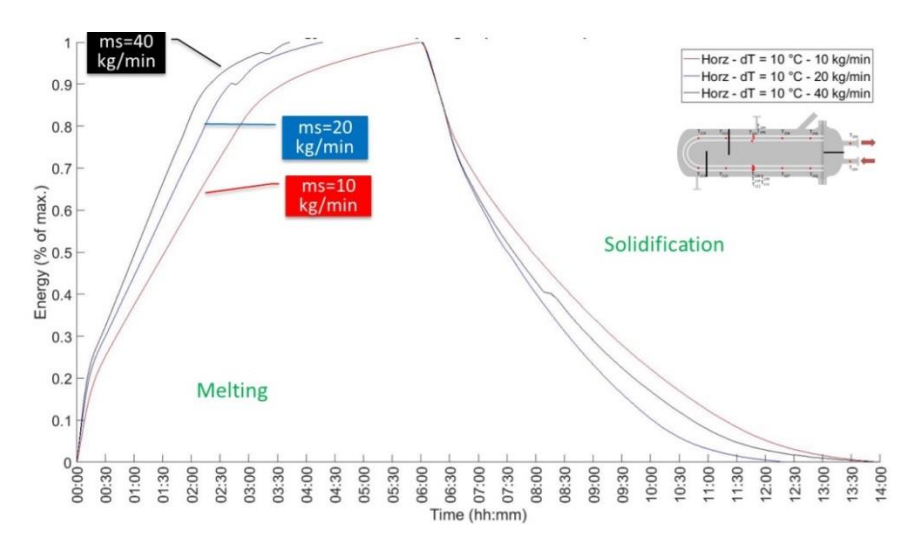


Figure 13: Effect of mass flow on energy content of storage for charging and discharging. Temperature difference is 10°C, vessel orientation is horizontal.

Finally, Figure 14 shows the effect of horizontal versus vertical orientation. In the measurements, a significantly higher thermal power was found for the horizontal configuration than for the vertical configuration, which is consistent with the faster charging of the storage as shown in the figure. The effect is particularly important for charging (melting), while for discharging (solidification) the effect is much less. This indicates that the effect is probably due to natural convection in the molten PCM. It is concluded that the horizontal orientation promotes effects of natural convection much more than the vertical orientation, which can be ascribed to the fact that in horizontal orientation, more and smaller convection cells will appear than in vertical orientation, and in addition, the convective flow is perpendicular to the tubes, instead of parallel to the tubes. Both these effects tend to increase the effectiveness of the natural convection heat transfer.

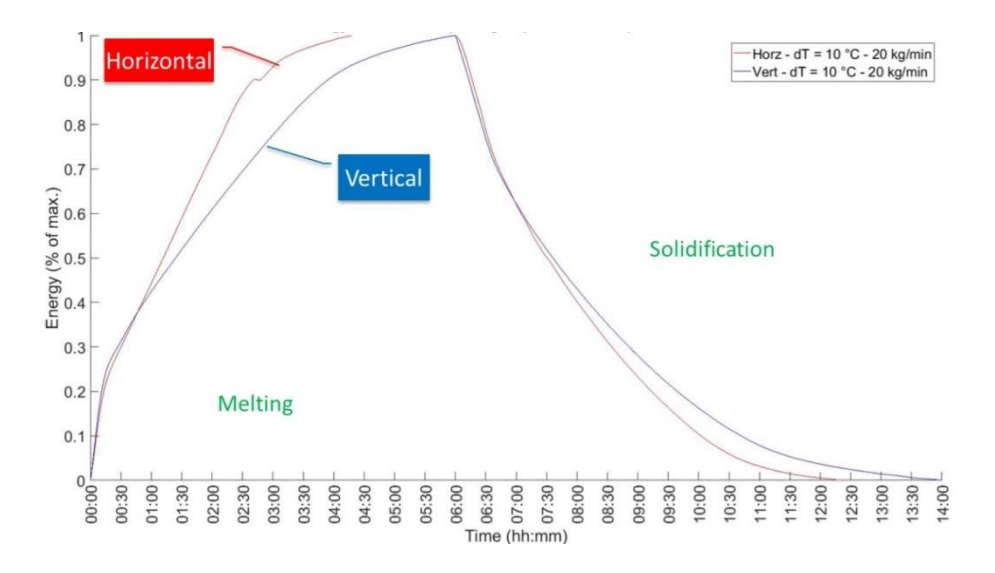


Figure 14: Effect of orientation on energy content of the storage. Temperature difference is 10°C, mass flow is 20 kg/min.

#### 5. Conclusions and outlook

A large scale lab prototype was built and compared to numerical model results. It was concluded that the model and the experimental results have a fairly good match, if the model contains a natural convection correction. Subsequently, the prototype was tested with different inflow temperatures, flow rates and orientations. It was found that temperature difference had an important effect on charge and discharge power, while the effect of flow rate (for the present design and measurement conditions) was less. A horizontal orientation was found to have a significantly higher charging power than a vertical geometry, which is ascribed to more effective natural convection in the molten PCM.

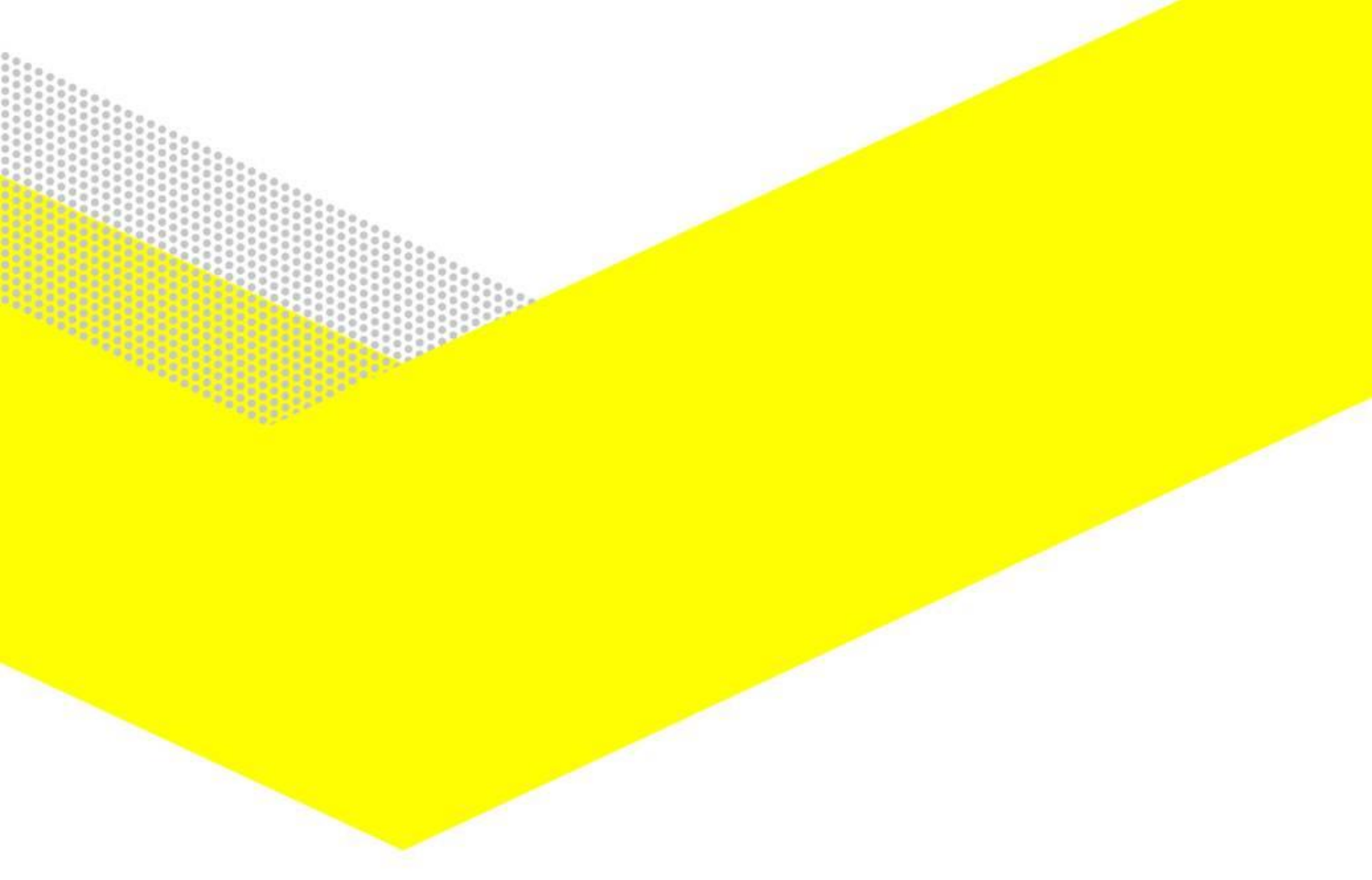
Next, the setup will be tested with MgCl<sub>2</sub>.6H<sub>2</sub>O as high temperature salt hydrate PCM. This PCM is seen as interesting for industrial applications, because of its high melting point of 117°C and the fact that it is a low cost material.

#### References

Mehling, H.; Cabeza, L. (2008), Heat and cold storage with PCM, Springer-Verlag, Berlin.

# Acknowledgements

The project is partially subsidized by the industrial energy savings program (EBI) of the Topsector Energy, nr. TEEI314008. The Netherlands Enterprise Agency (RVO.nl) is executing this program for the Institute for Sustainable Process Technology (TKI-ISPT).



#### **ECN**

Westerduinweg 3 P.O. Box 1
1755 LE Petten 1755 ZG Petten
The Netherlands The Netherlands

T +31 88 515 4949 F +31 88 515 8338 info@ ecn.nl www.ecn.nl